Membrane vesicles can contribute to cellulose degradation by *Teredinibacter turnerae,* a cultivable intracellular endosymbiont of shipworms

Mark T. Gasser[a]# | Annie Liu[a] | Marvin Altamia[b] | Bryan R. Brensinger[a] | Sarah L. Brewer[a] | Ron Flatau[b] | Eric R. Hancock[a] | Sarah P. Preheim[c] | Claire Marie Filone[a] | Dan L. Distel[b]#

[a]Johns Hopkins University Applied Physics Laboratory, Laurel, Maryland, USA 20723

[b]Ocean Genome Legacy Center, Northeastern University, Nahant, Massachusetts, USA 01908

[c]Johns Hopkins University, Baltimore, Maryland, USA 21218

Running title: Cellulolytic Membrane Vesicles from *T. turnerae*

Keywords: carbohydrate-active enzymes, CAZymes, lignocellulose degradation, OMVs, outer membrane vesicles, symbiosis, *tonB*-dependent receptors

MTG: mark.gasser@jhuapl.edu (ORCID: 0000-0002-9396-4954) #Co-corresponding author

AL: annie.liu@jhuapl.edu (ORCID: 0009-0002-3224-6008)

MAA: marvin.altamia@gmail.com (ORCID: 0000-0002-8625-767X)

BRB: bryan.brensinger@jhuapl.edu (ORCID: 0009-0002-0327-021X)

SLB: sarah.brewer@jhuapl.edu (ORCID: 0009-0007-9039-0784)

RF: r.flatau@northeastern.edu (ORCID: 0000-0002-4357-5870)

ERH: eric.hancock@jhuapl.edu (ORCID: 0009-0002-3041-2148)

SPP: sprehei1@jhu.edu (ORCID: 0000-0001-7365-2382)

CMF: claire.marie.filone@jhuapl.edu (ORCID: 0000-0002-4041-3948)

DLD: d.distel@northeastern.edu (ORCID: 0000-0002-3860-194X) #Co-corresponding author

Data availability

The authors confirm that the data supporting this study's findings are available within the article and its supplementary materials. The mass spectrometric raw files are accessible at https://massive.ucsd.edu under accession MassIVE MSV000094250 and at https://www.proteomexchange.org under accession PXD050419.

Funding statement

Research reported in this publication was supported by the following awards: National Oceanic and Atmospheric Administration (NA19OAR0110303), Gordon and Betty Moore Foundation (https://doi.org/10.37807/GBMF9339), National Institutes of Health (1R01AI162943-01A1, subaward: 10062083-NE) to DLD, and Johns Hopkins University Applied Physics Laboratory internal research and development funds to MTG and CMF. The National Science Foundation (DBI 1722553) also funded some equipment used in this research.

Conflict of interest statement

The authors report no conflict of interest. The funders had no role in study design, data collection, interpretation, or the decision to submit the work for publication.

Abstract

Teredinibacter turnerae is a cultivable cellulolytic Gammaproteobacterium (Cellvibrionaceae) that commonly occurs as an intracellular endosymbiont in the gills of wood-eating bivalves of the family Teredinidae (shipworms). The genome of *T. turnerae* encodes a broad range of enzymes that deconstruct cellulose, hemicellulose, and pectin and contribute to wood (lignocellulose) digestion in the shipworm gut. However, the mechanisms by which *T. turnerae* secretes lignocellulolytic enzymes are incompletely understood. Here, we show that *T. turnerae* cultures grown on carboxymethyl cellulose (CMC) produce membrane vesicles (MVs) that include a variety of proteins identified by LC-MS/MS as carbohydrate-active enzymes (CAZymes) with predicted activities against cellulose, hemicellulose, and pectin. Reducing sugar assays and zymography confirm that these MVs exhibit cellulolytic activity, as evidenced by the hydrolysis of CMC. Additionally, these MVs were enriched with *TonB*-dependent receptors, which are essential to carbohydrate and iron acquisition by free-living bacteria. These observations indicate a potential role for MVs in lignocellulose utilization by *T. turnerae* in the free-living state, suggest possible mechanisms for host-symbiont interaction, and may be informative for commercial applications such as enzyme production and lignocellulosic biomass conversion.

Introduction

The biological degradation of lignocellulose, a primary component of wood and all plant biomass, is a critical process in the global carbon cycle and has potential applications in renewable energy and chemical production through biomass conversion (Ragauskas *et al.*, 2014; Østby *et al.*, 2020). Lignocellulose is a complex composite material composed of microfibrils of cellulose, the most abundant organic polymer on Earth, embedded in a matrix of hemicellulose, pectin, and lignin (Cragg *et al.*, 2015; Dahmen *et al.*, 2019). However, due to the structural complexity of lignocellulose, its degradation typically requires multiple enzymes to disassemble and convert its component polymers into accessible nutrients. This complexity limits lignocellulose as a carbon source for most animals and creates obstacles to bioconversion to renewable fuels or fine chemicals (Cragg *et al.*, 2015). Nonetheless, many animals, including herbivores, termites, and wood-boring bivalves (shipworms), can digest lignocellulose in leafy or woody plant material with the aid of hydrolytic enzymes produced by symbiotic bacteria (Cragg *et al.*, 2015).

Bacteria use a variety of mechanisms to degrade lignocellulosic substrates. For example, polysaccharide-degrading bacteria, including *Bacteroides*, *Clostridia*, and *Fibrobacter,* commonly found in the gut microbiomes of ruminants*,* use the type IX secretion pathway (T9SS) to export large proteins, including multidomain carbohydrate-active enzymes (CAZymes) (Gharechahi *et al.*, 2023). These enzymes may be released into the environment or bound to the cell envelope (McGavin *et al.*, 1990; Cai *et al.*, 1999; Yan and Wu, 2013). Rumin bacteria may also export CAZymes via membrane vesicles (MVs) (Forsberg *et al.*, 1981; La Rosa *et al.*, 2022; Gharechahi *et al.*, 2023). MVs are membrane-enclosed spheres, typically 40-400 µM in diameter, that may form by blebbing or pinching off the outer membrane of diderm bacteria (Toyofuku *et al.*,

84 2023). MVs formed by this mechanism are called Outer Membrane Vesicles (OMVs) and contain
85 mainly periplasmic and outer membrane components (Guerrero-Mandujano *et al.*, 2017).
86 Bacteria may also form MVs by other mechanisms, resulting in MV types that contain
87 cytoplasmic membranes and other cytoplasmic components (Schwechheimer and Kuehn, 2015;
88 Nagakubo *et al.*, 2020; Huang *et al.*, 2022; Toyofuku *et al.*, 2023). Multiple MV types may be
89 produced simultaneously by the same bacterium (Gan *et al.*, 2023).
90 Bacterial MVs have been implicated in a wide variety of functions, including the export
91 of proteins, lipids, carbohydrates, metabolites, and nucleic acids; waste disposal; nutrient
92 scavenging; defense against phage and antibiotics; and delivery of bioactive molecules across
93 the plasma membranes of animal hosts (Toyofuku *et al.*, 2023). However, the extent to which
94 MVs contribute to bacterial lignocellulose degradation remains incompletely explored,
95 particularly in environments other than ruminant guts. In the rumen, members of several
96 bacterial phyla, including Fibrobacterota (Arntzen *et al.*, 2017), Bacilota (Ichikawa *et al.*, 2019),
97 and Bacteroidota (Forsberg *et al.*, 1981), produce MVs highly enriched in CAZymes capable of
98 degrading cellulose and other plant biomass. However, to our knowledge, no member of the
99 phylum Pseudomonadota (formerly Proteobacteria), the largest and most phenotypically
100 diverse bacterial phylum (Rosenberg *et al.*, 2014), has been shown to produce MV's with a
101 protein content that suggests specialization for degrading lignocellulose.
102 One example of an ecologically important lignocellulose-degrading Pseudomondadota
103 species is *Teredinibacter turnerae.* This gammaproteobacterium is a member of the family
104 Celvibrionaceae, which includes many polysaccharide-degrading marine bacteria (Spring *et al.*,
105 2015). *T. turnerae* is unusual in that it can exist either as a versatile free-living marine

106 lignocellulose-degrading bacterium (Distel *et al.*, 2002) or as an intracellular symbiont of
107 shipworms (Distel *et al.*, 1991), a family of bivalve mollusks that are the primary consumers of
108 wood in marine environments (Voight, 2015; Cragg *et al.*, 2020). Interestingly, unlike other
109 marine Cellvibrionaceae, the *T. turnerae* genome includes a broad representation of genes
110 associated with the degradation of terrestrial woody plant materials, including cellulose, xylan,
111 mannan, galactorhamnan and pectin, but lacks enzyme systems for degradation of common
112 marine polysaccharides including agar, alginate, and fucoidan and has only comparatively sparse
113 representation of chitinase and laminarinase genes (Yang *et al.*, 2009).

114 As a free-living bacterium, *T. turnerae* grows on both soluble and insoluble cellulosic
115 substrates, including carboxymethylcellulose (CMC), short-chain cellooligosaccharides,
116 cellobiose, purified cellulose, e.g., Sigmacell or Avicel cellulose), paper, e.g., Whatman #1 filter
117 paper (Waterbury *et al.*, 1983; Distel *et al.*, 2002), and crude plant biomass, e.g., pine sawdust,
118 cotton fiber, coconut hull fiber, and rice hulls (unpublished observation).

119 As an intracellular symbiont, *T. turnerae* grows within specialized cells called
120 bacteriocytes found in the gland of Deshayes, a tissue located within the shipworm's gills
121 (Popham and Dickson, 1973; Popham, 1974; Distel *et al.*, 1991). The genome of *T. turnerae* and
122 other shipworm symbionts from the genus *Teredinibacter* encode a wide variety of enzymes
123 targeting lignocellulose (Distel *et al.*, 2002; Yang *et al.*, 2009; O'Connor *et al.*, 2014; Brito *et al.*,
124 2018; Altamia *et al.*, 2020, 2021) and express them within this gland (O'Connor *et al.*, 2014;
125 Sabbadin *et al.*, 2018). Enzymes encoded in the shipworm symbiont's genomes are also found
126 in the shipworm's cecum (O'Connor *et al.*, 2014; Sabbadin *et al.*, 2018; Altamia and Distel,
127 2022). This gut compartment is a primary location of wood digestion in shipworms and is nearly

128 devoid of microbes (Betcher *et al.*, 2012). The distribution of symbiont-made enzymes in both
129 the intracellular environment of the host and in the gut, which is part of the host's external
130 environment, indicates the existence of an unusual and unexplained protein transport system
131 that potentially exports symbiont-made proteins across the host's cellular membranes (Altamia
132 and Distel, 2022).

133 While explaining the complex interaction of *T. turnerae* with its shipworm host is beyond
134 the scope of this investigation, understanding the mechanisms by which this bacterium exports
135 lignocellulolytic enzymes in the free-living state may shed light on potential mechanisms by
136 which these enzymes may be transported within its shipworm hosts. MVs are a versatile system
137 through which bacteria exchange proteins and other biomolecules with their external
138 environment and the internal environment of their hosts (Gan *et al.*, 2023; Toyofuku *et al.*,
139 2023). Therefore, we ask whether free-living cells of *T. turnerae* export lignocellulose-degrading
140 enzymes via MVs.

141 To address this question, we purify and characterize the protein composition of MVs
142 produced by *T. turnerae* during growth on carboxymethyl cellulose (CMC), a water-soluble
143 derivative of cellulose. We identified proteins in the purified MVs that are putatively involved in
144 interactions with lignocellulose by using LC-MS/MS analysis and comparison to the
145 Carbohydrate Active Enzyme Database (CAZy) (Lombard *et al.*, 2014). Additionally, we
146 performed activity assays to show that MVs produced by *T. turnerae* are capable of cellulose
147 hydrolysis. These observations suggest that MVs contribute to lignocellulose utilization by *T.*
148 *turnerae* in the free-living state and provide clues that might help explain enzyme transport
149 during host-symbiont interaction.

150 ## Experimental Procedures

151 ### Strain isolation, selection, and growth conditions

152 Two strains of *Teredinibacter turnerae* were selected for this study: *strain* T7901 (ATCC
153 39867; GenBank CP001614) and a closely related strain SR01903 (GenBank CP149818). The
154 former was isolated from the shipworm *Bankia gouldi* collected in Beaufort, NC, in 1979 and
155 was the first shipworm symbiont strain brought into pure culture (Waterbury *et al.*, 1983; Distel
156 *et al.*, 2002; Yang *et al.*, 2009). The latter was isolated from the gills of a single specimen of
157 *Lyrodus pedicellatus* found in naturally occurring driftwood collected by hand in shallow water
158 in the Indian River Lagoon, Merit Island, FL. (N 28.40605 W 80.66034) on January 24, 2020. Gills
159 were removed by dissection and homogenized in 1.0 ml of shipworm basal medium (SBM)
160 (Waterbury *et al.*, 1983) in an autoclave-sterilized glass dounce homogenizer. Homogenate was
161 streaked onto a culture plate containing 1.0% Bacto agar and SBM at pH 8.0 supplemented with
162 0.2% w/v powdered cellulose (Sigmacell Type 101; Sigma-Aldrich) and 0.025% NH_4Cl. Plates
163 were incubated at 30 °C until individual colonies could be observed. An individual colony was
164 then picked and subjected to multiple rounds of restreaking from single colonies to ensure
165 clonality. We PCR-amplified and sequenced the 16S rRNA gene to identify this isolate and
166 compared it to published *T. turnerae* genomes. The complete genome of *T. turnerae* SR01903
167 was then sequenced (SRA number SRR28421271) and submitted to Genbank (CP149818). For
168 the experiments described herein, strains were initially propagated in 6 mL cultures in SBM
169 supplemented with 0.025% NH_4Cl and 0.2% carboxymethyl cellulose for 4 days before being
170 diluted 1/250 in fresh media and harvested after 2 days (OD600 0.2-0.3). All cultures were
171 incubated in a shaker incubator at 30 °C and 100 rpm. An overview of the procedures conducted
172 in this research is presented in Figure 1.

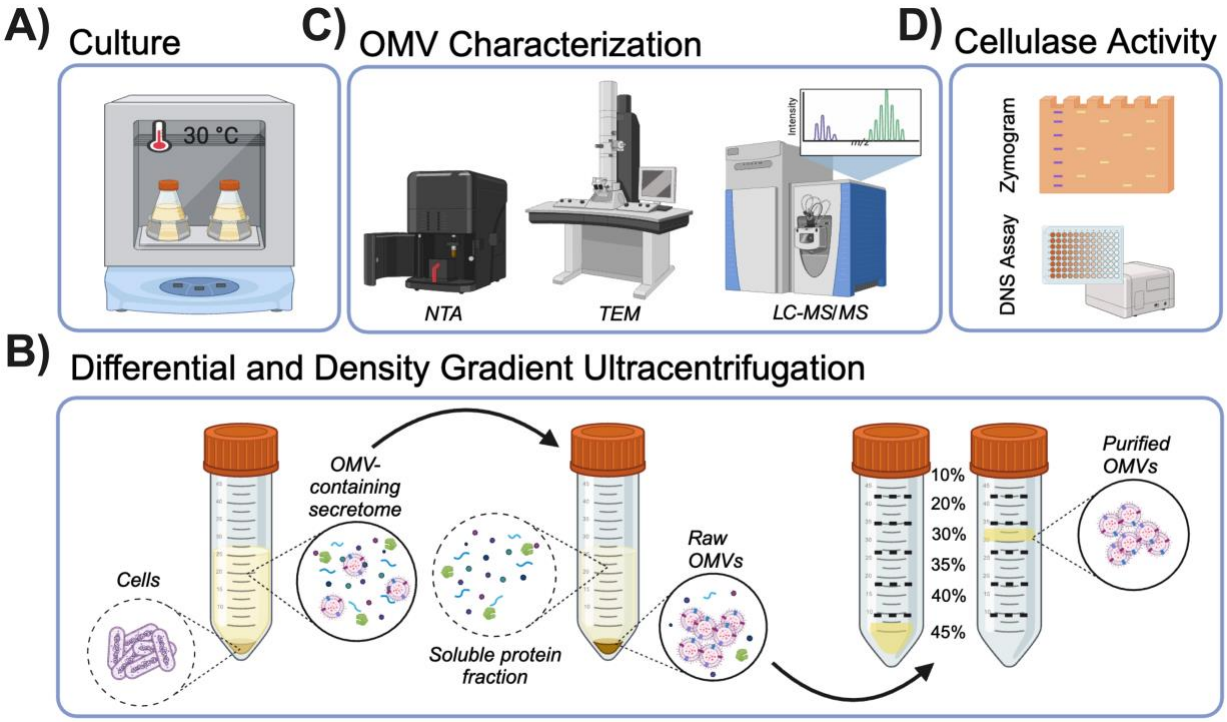

Figure 1. Methods used to isolate and characterize membrane vesicles (MVs) from T. turnerae. Diagram showing: (A) bacterial culture, (B) MV isolation based on differential and density gradient separation, (C) MV visualization and size determination by TEM and NTA, proteome analysis by LC-MS/MS, and (D) detection of cellulase activity in purified MV preparations by zymography and reducing sugar (DNS) assay. Created with BioRender.com

Isolation of Membrane Vesicles (MVs)

Bacterial cells were separated from the culture supernatant by centrifugation at 5,000 x g for 20 minutes at 4 °C. The supernatant was then transferred to a fresh tube, and centrifugation was repeated to remove residual bacterial cells. The final supernatant was carefully collected without disturbing the remaining pellet and filtered through a 0.22 µm polyethersulfone filter as an additional precaution to remove cells. The putative MVs were then pelleted from the filtrate by ultracentrifugation at 120,000 x g (T-647.5 rotor, Sorvall) for 90 minutes at 4 °C. For purification, the resulting pellet was resuspended in 0.1 M phosphate-buffered saline (PBS) and fractionated by bottom-up density gradient ultracentrifugation using Optiprep™ (iodixanol density gradient medium) as follows. The resuspended MV-containing pellet was mixed with 60% iodixanol solution to a final density of 45% (w/v) and placed at the

189 bottom of an ultracentrifuge tube. A discontinuous density gradient was generated using a
190 syringe and G21 needle to deposit 40%, 35%, 30%, 20%, and 10% iodixanol layers with a final
191 layer of 0.25 mL 0.1 M PBS on top. The resulting gradient was centrifuged for 16 hours at
192 150,000 x g and 4 °C (SW55 Ti rotor, Beckman-Coulter). Sample banding was visually observed
193 at the interface of the 30% and 20% fractions (Supporting Information: Figure S1). All fractions
194 were collected, and iodixanol was removed by passive diffusion dialysis (1,000 kDa MWCO) in
195 exchanging buffer of 50 mM ammonium bicarbonate pH 8.3 at 4 °C. MV samples were removed
196 from the dialysis bag and concentrated under vacuum to 100 µL (SPD121P SpeedVac, Thermo
197 Scientific). Particle visualization and characterization proceeded with the single 30% fraction.

198 Transmission electron microscopy (TEM)

199 Purified MVs were diluted in molecular grade distilled water and absorbed onto 200
200 mesh formvar-treated and carbon-coated copper grids for 60 seconds. Samples were then fixed
201 for 5 minutes in 4% glutaraldehyde in 0.1 M sodium cacodylate, and grids were negatively
202 stained with 1% aqueous uranyl acetate for 60 seconds and left to dry. MVs were imaged in an
203 FEI Tecnai T12 (Thermo Fisher) transmission electron microscope at 80 kV with an AMT bottom-
204 mount camera.

205 Nanoparticle tracking analysis (NTA)

206 NTA was performed using the ZetaView® PMX-220 Twin (Particle Metrix) configured with
207 488 nm and 640 nm lasers with long wave-pass cut-off filters (500 nm and 660 nm, respectively)
208 and a sensitive CMOS camera 640 x 480 pixels. Samples were diluted in 2 mL of 0.1 µm filtered
209 deionized water (18 MΩ/cm) to obtain a particle concentration between 1×10^7 and 1×10^8
210 particles/mL. The instrument was set to a sensitivity of 80, a shutter speed of 100, and a frame
211 rate of 30 frames per second. Each sample was measured at 11 different positions throughout

212 the sample cell, with 1 cycle of reading at each position to have a minimum of 1,000 traces. If
213 the number of traces was below 1,000 counts, some additional sample was flushed inside the
214 sample cell, and the acquisition was repeated. Post-acquisition parameters were set to a
215 minimum brightness of 20, a maximum size area of 1,000 pixels, a minimum size area of 10
216 pixels, and tracelength of 15 frames. Automated cell quality control was checked using high-
217 quality deionized water. Camera alignment and focus optimization were performed using
218 polystyrene Nanosphere™ 100 nm size standard beads. Data analysis was performed with
219 ZetaView® 8.05.14 software provided by the manufacturer. Automated reports of the particle
220 recordings across the 11 positions were manually checked, and any outlier position was
221 removed to calculate particle concentration and distribution.

222 ### Proteomic analysis

223 MVs were lysed and denatured in a solution containing 5% sodium dodecyl sulfate (SDS),
224 100 mM Tris (pH=8), 20 mM chloroacetamide, and 10 mM tris (2-carboxyethyl) phosphine
225 hydrochloride and incubated at 90 °C for 10 minutes. Proteins were aggregated and isolated
226 using Sera-Mag™ carboxylate-modified SpeedBeads (SP3 beads) and digested in 100 mM
227 NH_4HCO_3 containing Trypsin (final concentration 6 ng/µL) overnight at 37 °C and 1,200 rpm.
228 Digested samples were loaded onto C18 tips, and peptides were separated online using an 88-
229 minute LC gradient (Evosep LC system). MS analysis was performed on a Q-Exactive HF-X Hybrid
230 Orbitrap mass spectrometer (Thermo Scientific). One full high-resolution MS spectrum was
231 acquired with a resolution of 45,000, an AGC target of 3×10^6 with a maximum ion time of 45
232 ms, and a scan range of 400-1,500 m/z, followed by 20 HCD MS/MS scans with a resolution of
233 1,5000, an AGC target of 1×10^5 with a maximum ion time of 120 ms, NCE of 27, and isolation
234 window of 2 m/z. The resulting MS/MS spectra were searched against the strain-specific and

235 universal contaminant protein databases using Sequest within Proteome Discoverer 1.4.

236 Identifications were filtered to include only high-confidence peptides based on a less than 1%

237 false discovery rate (FDR) against a decoy database. FDR estimates the expected ratio of false

238 positive classifications (false discoveries) to total positive classifications. Proteins were linked to

239 peptides, and only proteins with >2 peptide spectral matches (PSM) with two unique peptides

240 were kept (Supporting Information: Dataset S1).

241 Functional characterization of MV proteins

242 Identified proteins were annotated against the Clusters of Orthologous Groups (COG) of

243 proteins database (Galperin *et al.*, 2021). Additionally, protein subcellular locations and

244 secretion signals were predicted using DeepLocPro v1.0

245 (https://services.healthtech.dtu.dk/services/DeepLocPro-1.0/) (Moreno *et al.*, 2024) and Signal

246 v5.0 (https://services.healthtech.dtu.dk/services/SignalP-5.0/) (Almagro Armenteros *et al.*,

247 2019), respectively. Enrichment and functional associations between proteins were

248 determined by STRINGdb v11 (https://string-db.org/) (Szklarczyk *et al.*, 2019) and ShinyGO v0.8

249 (http://bioinformatics.sdstate.edu/go/) (Ge *et al.*, 2018). Settings were selected to use all coding

250 sequences in the T7901 genome as background and a minimum FDR stringency of 1×10^{-5}. We

251 then established which MV proteins are predicted to exhibit carbohydrate-active properties

252 using the annotated T7901 genome in the Carbohydrate Active Enzymes Database (CAZy,

253 https://cazy.org) (Lombard *et al.*, 2014).

254 Enzymatic activity assays

255 The cellulolytic activity of proteins in MV preparations was visualized and size

256 fractionated by denaturing polyacrylamide gel electrophoresis (SDS-PAGE, 1.5 mm thickness, 9%

257 acrylamide, and 0.2% CMC final concentration). For zymographic analysis, 14 µg of protein

258 sample determined by Pierce 660 assay (Thermo Scientific) using bovine serum albumin as
259 standard were heat denatured by boiling for 3 minutes in SDS without a reducing agent to
260 facilitate recovery of activity after refolding and added to each lane. After electrophoresis, the
261 SDS-PAGE gel was transferred to 500 mL of refolding buffer (20% isopropanol, 0.1% Triton X-100
262 in 1x PBS, pH 7.4) and gently shaken for 1 hour at room temperature. The gel was then
263 incubated in fresh 1x PBS buffer, pH 7.4, for 16 hours at room temperature before being stained
264 with 0.1% Congo Red in 1x PBS buffer, pH 7.4 for 1 hour. The zymogram was destained with 1 M
265 NaCl overnight to visualize regions where cellulase activity removed CMC.

266 Additionally, the production of reducing ends was measured by the colorimetric 3,5-
267 dinitrosalicylic acid (DNS) method (Ghose, 1987). Reactions were carried out in 96-well plates
268 containing 50 µL 1% CMC, 30 µL 50 mM citrate buffer, and 20 µL purified MV suspension and
269 incubated for 4 hours at 37 °C. Next, 900 µL of DNS was added to each reaction, and reactions
270 were heated at 99 °C for 10 minutes. Absorbance was measured at 540 nm, and sugar
271 concentration was calculated by comparison to a glucose standard curve. The enzyme activity
272 unit was defined as the amount of enzyme that liberated 1 µmol of reducing sugar per minute.

273 Results

274 MV isolation and characterization

275 MVs were isolated from cell-free supernatants of two closely related strains of *T.*
276 *turnerae*, T7901 and SR01903, by density gradient ultracentrifugation. The presence of MVs was
277 confirmed by NTA and TEM (Figure 2 A-D). The mean concentration of particles and average
278 particle diameter determined by NTA were 1.67 x 10^9 particles/mL and 162.5 $\pm$ 49.7 nm for
279 T7901 and 1.30 x 10^9 particles/mL and 206.6 $\pm$ 61.7 nm for SR01903. TEM images (Figure 2 C-D)

280 show that the putative MV-enriched fractions from strains T7901 and SR01903 contain particles

281 with size distribution and morphology typical of bacterial MVs.

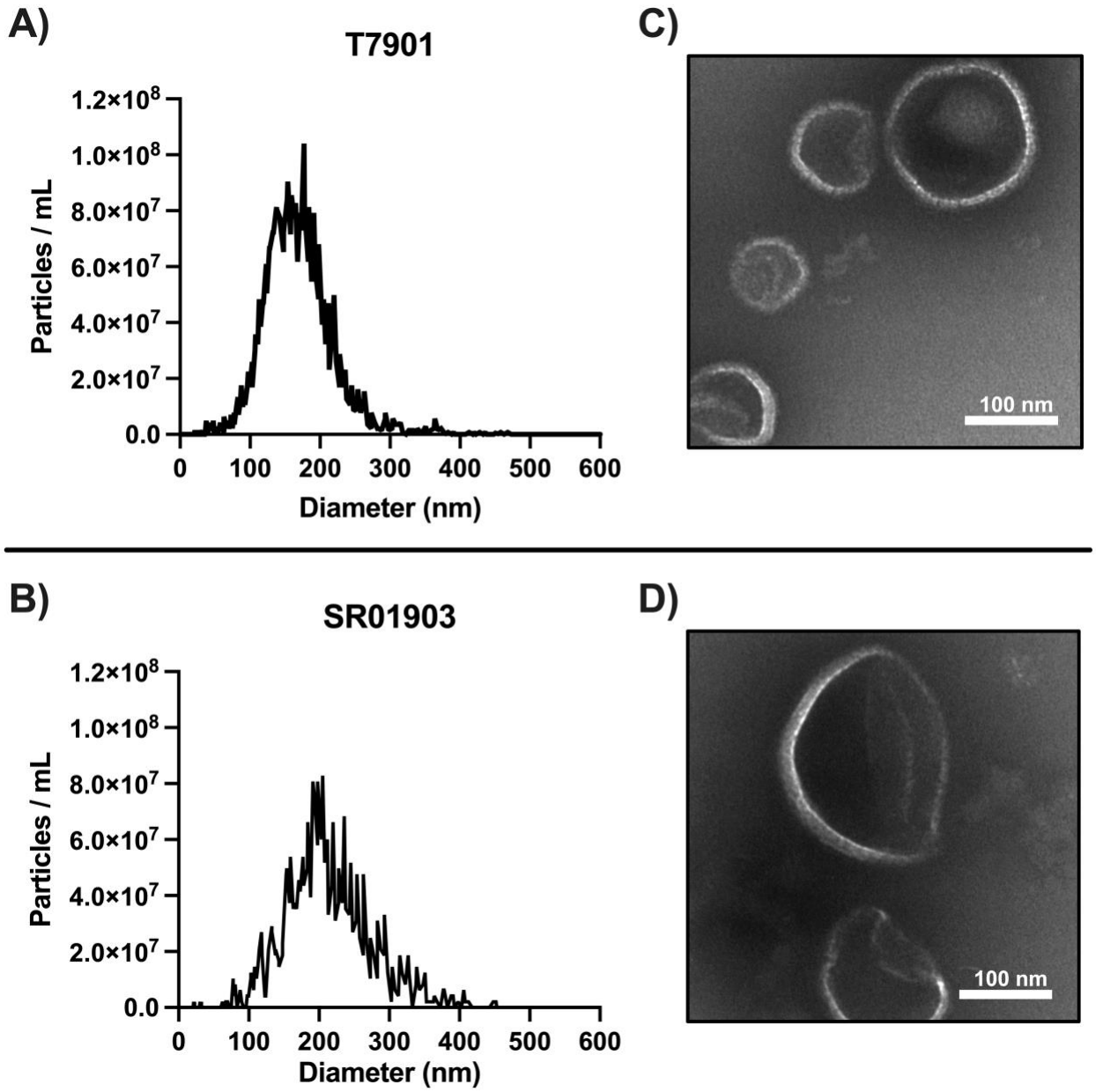

282

283 *Figure 2. Size, concentration, and visualization of MVs isolated from T. turnerae culture supernatants after growth on*
284 *carboxymethyl cellulose (CMC). (A-B) Size distribution and particle concentration for strains T7901 and SR01903, respectively.*
285 MVs from SR01903 were slightly larger in average size than MVs from T7901. *(C-D) Isolated MVs from strains T7901 and*
286 *SR01903, respectively, were imaged using transmission electron microscopy. Scale bar = 100 nm.*

287 ## MV proteome analysis

288 The protein content of MVs from *T. turnerae* strains T7901 and SR01903 were analyzed
289 by LC-MS/MS. Peptide-generated data were used to search against T7901 and SR01903
290 annotated protein sequences to identify MV proteins and their relative abundance. A cut-off of
291 two or more unique predicted peptides per identified protein was used, identifying 472 and 569
292 proteins for T7901 and SR01903, respectively. The Top 100 most abundant proteins identified in
293 T7901 and SR01903 represented 81% and 74% of the total peptide content, respectively. Among
294 those proteins, 71 were identified in both strains, indicating that the two strains produce a
295 shared core set of MV proteins when grown under the examined culture condition. After
296 protein identification, DeepLocPro v1.0 (Moreno *et al.*, 2024) and Signal v5.0 (Almagro
297 Armenteros *et al.*, 2019) were used to predict the subcellular location and secretion signals of
298 all identified proteins.

299 Outer membrane proteins comprised most (~76% and ~71%, respectively) of the MV
300 protein mass of both T7901 and SR01903 (Figure 3 A). Although cytoplasmic and inner
301 membrane proteins were detected, these constituted only about 9% of total protein by mass.
302 This indicates that these MV preparations were mainly comprised of outer membrane vesicles
303 but may have contained other types, e.g., outer inner membrane vesicles (OIMVs) (Toyofuku *et*
304 *al.*, 2023).

305 MV proteins were clustered into orthologous groups (COG). Most MV proteins assigned
306 to clusters in both strains were categorized as Cell Wall/Membrane/Envelope Biogenesis,
307 Inorganic Ion Transport and Metabolism, and Carbohydrate Transport and Metabolism (Figure 3
308 B).

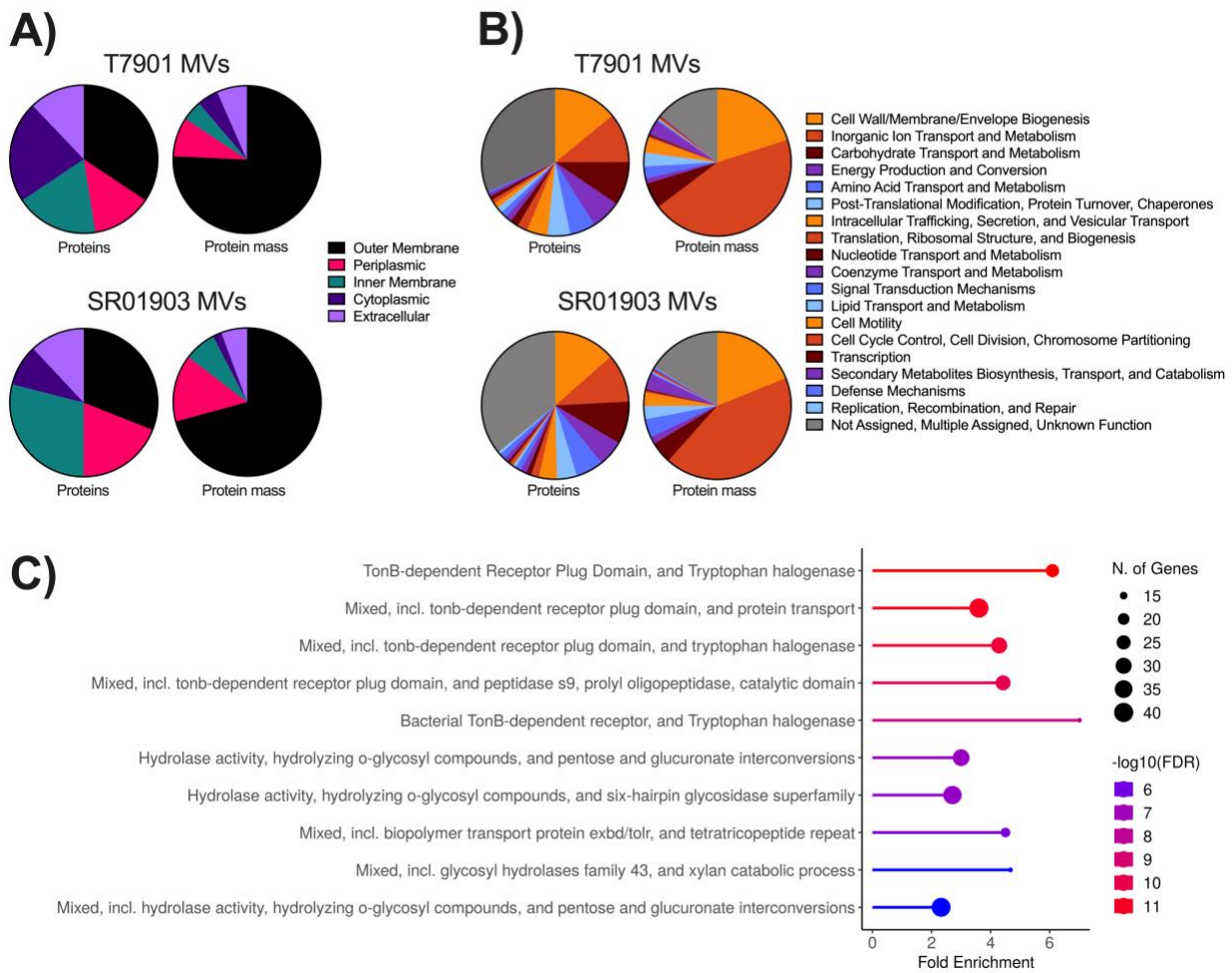

Figure 3. T. turnerae MV proteome profiles. (A) Relative protein abundance grouped by predicted subcellular location and (B) Clusters of Orthologous Groups (COG) functional categories of identified proteins. Six color-safe hues represent COG categories and are repeated in order starting from 12 o'clock on the graph and moving clockwise. (C) Top 10 STRINGdb pathways ranked by false discovery rate (FDR) found in MVs of T7901. Similar top pathways were found in the MVs of SR01903. STRING analysis was performed against the corresponding bacterial strain genome background to estimate the amount or fold of enrichment, i.e., the representation of that functional category above what is expected by chance. FDR estimates the expected ratio of false positive classifications (false discoveries) to total positive classifications.

TonB-dependent receptors and glycosyl hydrolase activity are enriched in MVs

MV protein content was analyzed using STRING (Szklarczyk *et al.*, 2019) enrichment to highlight functional associations. We found significant enrichment of pathways involving *TonB*-dependent receptors (TBDR) and glycosyl hydrolase activity (Figure 3 C). The most abundant proteins were TBDRs, which constituted ~47% and ~44% of the MV protein content by mass in T7901 and SR01903, respectively. In total, 39 and 48 predicted CAZymes were present,

324 representing 30 and 29 different catalytic CAZy families and 8.3% and 8.4% of identified MV
325 proteins in T7901 and SR01903, respectively. Most identified CAZy modules belong to glycoside
326 hydrolase families (GH) predicted to be involved in cellulose and hemicellulose degradation
327 (Figure 4 A) and that include several hydrolytic activities: for example, endo-glucanases (GH5,
328 GH8, GH9, GH10, GH11, GH26, GH44, GH45, GH51, GH62), exo-glucanases (GH5, GH9, GH26,
329 GH43), and beta-glucosidases (GH2, GH3, GH5, GH39). In addition, multiple enzymes were
330 predicted to include non-catalytic carbohydrate-binding modules (CBMs), with predicted
331 specificity for cellulose or hemicellulose components.

332 ## Cellulase activity

333 Many MV proteins were predicted to have or be associated with cellulolytic activity. We
334 confirmed these by testing MV suspensions for hydrolytic activity against CMC by zymography
335 and reducing sugar DNS assay. In zymograms, clear zones indicating endoglucanase activity
336 (Teather and Wood, 1982) were visualized between 95-130 kDa for both strains after 16-hour
337 incubation (Figure 4 B). The production of reducing sugars from CMC was measured using DNS
338 assay, and when normalized to total protein content, MVs produced from SR01903 displayed
339 similar or significantly greater cellulolytic activity compared to a commercial soluble cellulase
340 enzyme cocktail (Figure 4C). Notably, MVs produced from T7901 showed ~10x the activity of the
341 commercial cellulase cocktail (Figure 4 C) against CMC. While we observed a substantial
342 difference in CMC hydrolysis between MVs from the two *T. turnerae* strains, the ecological and
343 physiological significance of this difference is difficult to interpret as CMC is not a naturally
344 occurring substrate, and we did not control for differences in the density beyond OD600
345 measurement or physiological state of cells at the time of MV purification.

346

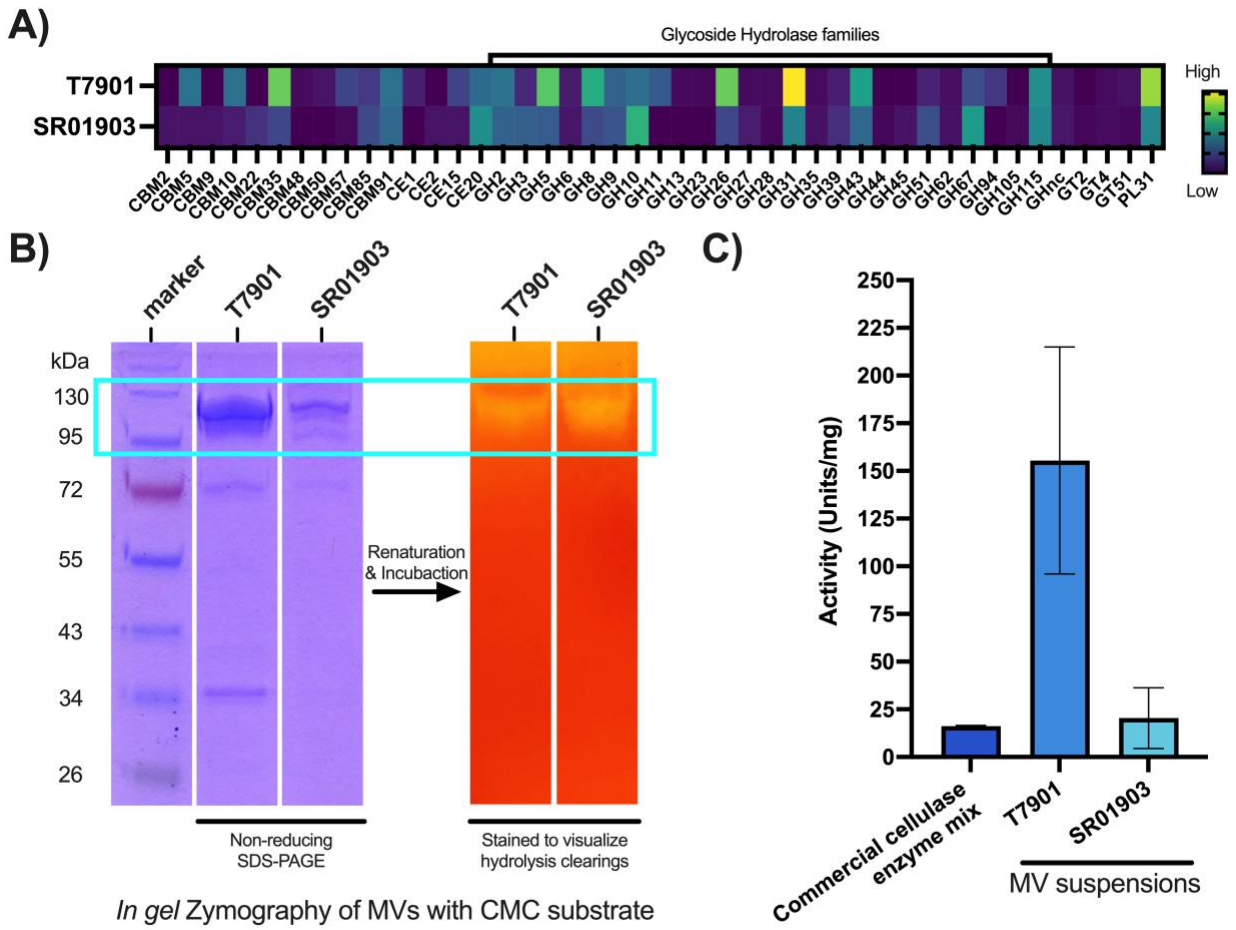

Figure 4. Occurrence and relative abundance of carbohydrate-active modules and detection of cellulase activity in T. turnerae MVs. (A) Heatmap profile of the relative abundance of the predicted carbohydrate-active enzymes found in MVs. (B) Denaturing nonreducing SDS-PAGE (left) and zymogram (right; CMC substrate) of isolated MVs. (C) Histogram showing cellulase activity (CMC substrate) in Units/mg (as determined by DNS assay) for isolated MVs and a purified cellulase enzyme cocktail (Cellulase R-10, Goldbio CAS# 9012-54-8). Bars indicate means (error bars: standard deviations of three replicates).

Discussion

MVs in bacterial lignocellulose degradation

The extent to which bacterial MVs contribute to lignocellulose degradation and the types of bacteria that produce lignocellulolytic MVs have been investigated in gut microbiomes (Forsberg *et al.*, 1981; McGavin *et al.*, 1990; Elhenawy *et al.*, 2014; Burnet *et al.*, 2015; Arntzen *et al.*, 2017; La Rosa *et al.*, 2022; Gharechahi *et al.*, 2023) but are less well explored in other organisms and environments. In bacteria, efficient deconstruction of lignocellulose typically requires multiple carbohydrate-active enzymes (CAZymes), each of which may contain multiple

361 catalytic and carbohydrate-binding modules. These catalytic modules encompass a broad range
362 of enzymatic activities. Glycoside hydrolase (GH) modules may have endo- or exo-activities
363 targeting the inner or terminal bonds of cellulose and hemicellulose backbones, as well as
364 activities targeting the oligomers and monomers that constitute cellulose and hemicellulose.
365 Carbohydrate esterase (CE) modules cleave bonds that form hemicellulose side chains and
366 bonds between hemicellulose and lignin. Carbohydrate binding modules (CBMs) adhere to
367 various carbohydrate components of lignocellulose and can enhance enzyme activity by
368 increasing accessibility to the substrate (Hervé *et al.*, 2010).

369 Packaging of lignocellulose-degrading CAZymes within MVs or bound to MV surfaces can
370 have distinct advantages over their secretion as soluble proteins or proteins bound to the cell
371 surface. For example, MVs may protect proteins from degradation (Bonnington and Kuehn,
372 2014; Alves *et al.*, 2016; Zingl *et al.*, 2021), selectively concentrate proteins with specific
373 functions (Orench-Rivera and Kuehn, 2016; Sartorio *et al.*, 2023), and deliver proteins to remote
374 locations in sufficient quantity to produce a desired effect without the dilution that soluble
375 proteins would experience (Toyofuku *et al.*, 2023). These factors may be significant for the
376 degradation of complex and insoluble substrates like lignocellulose, where the simultaneous
377 delivery of specific sets of catalytic and carbohydrate-binding modules in the correct
378 proportions and spatial orientation can yield significant synergistic interactions and enhance
379 efficiency (Park *et al.*, 2014).

380 Despite these advantages and the ubiquitous production of MVs by bacteria, members
381 of only a few bacterial phyla, notably Fibrobacterota (Arntzen *et al.*, 2017), Bacilota (Ichikawa *et*
382 *al.*, 2019), and Bacteroidota (Forsberg *et al.*, 1981), have been shown to produce MVs capable

383 of deconstructing lignocellulose. Here, we report that *Teredinibacter turnerae*
384 (Pseudomonadota; Gammaproteobacteria; Cellvibrionacea) produces MVs containing a wide
385 variety of enzymes with predicted activity against lignocellulose and that cellulolytic activity is
386 retained by MVs upon purification.

387 Among Pseudomonadota, several species package carbohydrate-active enzymes in MVs,
388 many of which target marine plant polysaccharides. For example, when grown on k-
389 carrageenan, the marine gammaproteobacterium *Alteromonas macleodii* produces MVs
390 enriched in CAZymes (Naval and Chandra, 2019). These include GH16, a family whose members
391 are active against multiple marine plant polysaccharides, including agar, k-carrageenan, and
392 porphyrin, GH28 which includes mainly polygalacturonases, and GH42, which are mostly B-
393 galactosidases (Naval and Chandra, 2019). Similarly, *Pseudoalteromonas distincta* produces MVs
394 with predicted hydrolytic activity against pectin and alginate (Dürwald *et al.*, 2021).

395 MVs may also contain enzymes active against components of lignocellulose. For
396 example, the plant pathogen *Xanthomonas campestris* produces MVs containing two virulence-
397 associated xylanases involved in pathogenic infection (Solé *et al.*, 2015). In *Pseudomonas*
398 *putida*, MVs play a role in the degradation of lignin-derived aromatic monomers but not
399 oligomeric lignin (Choi *et al.*, 2014; Salvachúa *et al.*, 2020).

400 Lignocellulolytic MVs produced by *T. turnerae*

401 When grown in pure culture and within the gills of its shipworm hosts, *T. turnerae*
402 secretes a broad array of CAZymes that specifically target lignocellulose (Yang *et al.*, 2009;
403 O'Connor *et al.*, 2014; Sabbadin *et al.*, 2018). However, the role of MVs in transporting
404 cellulolytic enzymes by *T. turnerae* has not been investigated. Here, we show that

405 lignocellulolytic CAZymes constituted a substantial proportion of the MV proteomes of *T.*
406 *turnerae* strains T7901 and SR01903 (8% and 6% by count and 8% and 5% by mass,
407 respectively). Of these, 94% have predicted secretion signals, and 43% are predicted to be
408 lipoproteins anchored to the outer membrane by a lipid moiety. Detected MV proteins included
409 representatives of 11 carbohydrate-binding module (CBM) families (CBM2, 5, 9, 10, 22, 35, 48,
410 50, 57, 85, and 91). Each of these families is known to bind cellulose or hemicellulose
411 components, except for CBM50, which typically binds peptidoglycan or chitin. Additionally,
412 catalytic modules representing 23 glycoside hydrolase (GH) families, four carbohydrate esterase
413 (CE) families, and one polysaccharide lyase (PL) were detected. All of these GH families (GH2, 3,
414 5, 8, 9, 10, 11, 13, 23, 26, 28, 31, 35, 39, 43, 44, 45, 51, 62, 67, 94, 105, and 115) target bonds
415 found within cellulose, hemicellulose or pectin, except GH23, which primarily acts on
416 peptidoglycan. Finally, the four carbohydrate esterase (CE) families detected (CE1, 2, 15, and 20)
417 target bonds found in hemicellulose, or bonds covalently linking hemicellulose to lignin. Thus,
418 bioinformatic predictions indicate the ability of *T. turnerae* MVs to hydrolyze a wide range of
419 bonds in lignocellulose, including potential endo- and exo-activities against cellulose and
420 hemicellulose backbones, debranching of hemicellulose sidechains, and hydrolysis of the
421 resulting oligomers and monomers.
422 The fact that this wide array of activities was found in MVs produced by cells of *T.*
423 *turnerae* strains T7901 and SR01903 grown with pure CMC as a sole carbon source indicates
424 that the expression of genes active against other lignocellulose components was either
425 constitutive or co-regulated with expression of genes targeting cellulose. The ability of *T.*
426 *turnerae* to express these activities in the absence of induction by their specific target

427 substrates is consistent with the observation that shipworm endosymbionts express a wide
428 range of lignocellulolytic enzymes when growing within symbiont-containing cells
429 (bacteriocytes) in the gill of the host where they have no direct contact with lignocellulose
430 (O'Connor *et al.*, 2014; Sabbadin *et al.*, 2018).

431 In addition to proteomic predictions, we show that these MV preparations can hydrolyze
432 CMC with specific activities comparable to or greater than that observed for a commercial
433 purified cellulase enzyme cocktail (Figure 4 C). Although CMC is not cleaved by all cellulolytic
434 enzymes, hydrolysis of CMC confirms that at least some of the detected cellulases retain their
435 activity in purified MVs.

436 ### TonB-dependent receptors in *T. turnerae* MVs

437 Although CAZymes constitute a substantial proportion of *T. turnerae* MV proteomes, the
438 most abundant proteins observed in MV preparations were identified as TonB-dependent
439 receptors (TBDRs). As previously reported in MVs of several Gram-negative bacteria (Veith *et al.*,
440 2015; Zakharzhevskaya *et al.*, 2017; Dhurve *et al.*, 2022; Fadeev *et al.*, 2023), TBDRs account for
441 nearly half of the proteins detected in *T. turnerae* MVs. TBDRs are outer membrane-associated
442 proteins that bind and mediate the energy-dependent movement of siderophores and various
443 nutrients, including polysaccharides too large to be taken up via transmembrane diffusion
444 across the outer membrane. Recently, it was shown that two of *T. turnerae's* four *TonB* genes
445 are essential for growth in iron-limiting conditions and for growth with cellulose as a sole
446 carbon source, indicating that the *TonB* system (TBDR and *TonB*) is necessary for both iron
447 acquisition and cellulose catabolism by *T. turnerae* (Naka and Haygood, 2023).

448 Interestingly, in a proteomic examination of the shipworm *Banka setacea*, a TBDR was
449 the only major symbiont-derived protein observed in the cecum content that was not
450 associated with the decomposition of lignocellulose (O'Connor *et al.*, 2014). This finding
451 suggests the presence of symbiont outer membranes in the cecum. However, the cecum of
452 shipworms has been shown by microscopic (Betcher *et al.*, 2012; Pesante *et al.*, 2021),
453 transcriptomic (Sabbadin *et al.*, 2018), and proteomic (O'Connor *et al.*, 2014) methods to be
454 nearly devoid of intact bacterial cells. These observations argue against the transport of whole
455 bacterial cells from the gill to the cecum, as suggested by (Pesante *et al.*, 2021), but might
456 suggest a role for MVs in transporting lignocellulose degrading enzymes from the gill to the gut
457 in shipworms.

458 ## Roles of MVs in symbiotic associations

459 Membrane vesicles are critical in bacterial interactions with many animal and plant hosts
460 (Berleman and Auer, 2013; Lynch and Alegado, 2017). While most research has focused on
461 pathogenic interactions (Gan *et al.*, 2023), MVs may also contribute to beneficial host-symbiont
462 associations. For example, MVs have been shown to mimic whole cells of *Vibrio fisheri* in the
463 induction of specific aspects of light organ development in the Hawaiian bobtail squid *Euprymna*
464 *scolope* (Aschtgen *et al.*, 2016). Similarly, bacterial MVs significantly promoted the settlement of
465 marine sponge larvae (Zhang *et al.*, 2024). MVs are also produced by chemoautotrophic
466 symbionts that occur in the trophosome of flatworms of the genus *Paracatenula,* where they
467 play a critical role in providing the host with carbohydrates synthesized by the symbionts (Jäckle
468 *et al.*, 2019).

469 ## Potential role of MVs in biomass conversion

470 In addition to their potential roles in shipworm symbiosis, cellulolytic MVs are of
471 significant interest in converting plant biomass into renewable liquid fuels or fine chemicals
472 (Thakur *et al.*, 2023). A significant challenge in biomass conversion is understanding how
473 cooperation among cellulases and associated enzymes can improve the design of efficient
474 enzyme cocktails tailored to individual feedstocks (Østby *et al.*, 2020). MVs produced by *T.*
475 *turnerae* and other lignocellulolytic organisms may represent nature-based solutions that reveal
476 specific combinations, concentrations, and spatial organization of cooperating enzymes that
477 significantly enhance lignocellulose degradation in nature and so might inspire the design of
478 engineered lignocellulose deconstruction systems.
479

480 ## Figure legends

481 Figure 1. Methods used to isolate and characterize membrane vesicles (MVs) from *T. turnerae*.
482 Diagram showing: (A) bacterial culture, (B) MV isolation based on differential and
483 density gradient separation, (C) MV visualization and size determination by TEM and
484 NTA, proteome analysis by LC-MS/MS, and (D) detection of cellulase activity in purified
485 MV preparations by zymography and reducing sugar (DNS) assay. Created with
486 BioRender.com

487 Figure 2. Size, concentration, and visualization of MVs isolated from *T. turnerae* culture
488 supernatants after growth on carboxymethyl cellulose (CMC). (A-B) Size distribution
489 and particle concentration for strains T7901 and SR01903, respectively. MVs from
490 SR01903 were slightly larger in average size than MVs from T7901. (C-D) Isolated MVs
491 from strains T7901 and SR01903, respectively, were imaged using transmission
492 electron microscopy. Scale bar = 100 nm.

493 Figure 3. T. turnerae MV proteome profiles. (A) Relative protein abundance grouped by
494 predicted subcellular location and (B) Clusters of Orthologous Groups (COG) functional
495 categories of identified proteins. Six color-safe hues represent COG categories and are
496 repeated in order starting from 12 o'clock on the graph and moving clockwise. (C) Top
497 10 STRINGdb pathways ranked by false discovery rate (FDR) found in MVs of T7901.
498 Similar top pathways were found in the MVs of SR01903. STRING analysis was
499 performed against the corresponding bacterial strain genome background to estimate
500 the amount or fold of enrichment, i.e., the representation of that functional category
501 above what is expected by chance. FDR estimates the expected ratio of false positive
502 classifications (false discoveries) to total positive classifications.
503 Figure 4. Occurrence and relative abundance of carbohydrate-active modules and detection of
504 cellulase activity in *T. turnerae* MVs. (A) Heatmap profile of the relative abundance of
505 the predicted carbohydrate-active enzymes found in MVs. (B) Denaturing nonreducing
506 SDS-PAGE (left) and zymogram (right; CMC substrate) of isolated MVs. (C) Histogram
507 showing cellulase activity (CMC substrate) in Units/mg (as determined by DNS assay)
508 for isolated MVs and a purified cellulase enzyme cocktail (Cellulase R-10, Goldbio CAS#
509 9012-54-8). Bars indicate means (error bars: standard deviations of three replicates).
510

511 ## Author Contribution Statement

512 **Mark T. Gasser:** Conceptualization; investigation; formal analysis; methodology; writing –
513 original draft preparation. **Annie Liu:** Investigation; methodology. **Marvin A. Altamia:**
514 Investigation; methodology. **Bryan R. Brensinger:** Investigation; methodology. **Sarah L. Brewer:**
515 Investigation; methodology. **Ron Flatau:** Investigation; methodology. **Eric R. Hancock:**

516 Investigation; methodology. **Sarah P. Preheim:** Supervision; writing – review and editing. **Claire**
517 **Marie Filone:** Funding acquisition; supervision; writing – review and editing. **Dan L. Distel:**
518 Funding acquisition; Conceptualization; supervision; writing – original draft preparation; writing
519 – review and editing.
520

521 ## Acknowledgments

522 We thank the PennVet Extracellular Vesicle Core SCR_022444 (Philadelphia, Pennsylvania) for
523 work and assistance with MV isolation and NTA analysis; the University of Maryland School of
524 Medicine's and School of Dentistry's Electron Microscopy Core Imaging Facility - EMCIF
525 (Baltimore, Maryland) for work and assistance with TEM imaging; and the NYU Langone's
526 Proteomics Laboratory SCR_017926 (New York, New York) for work and help with mass
527 spectrometry analysis.
528

529 ## Supplemental Information

530 Figure_S1_SuppInfo.docx
531 Dataset_S1_SuppInfo.xlsx
532

533 ## References

534 Almagro Armenteros, J.J., Tsirigos, K.D., Sønderby, C.K., Petersen, T.N., Winther, O., Brunak, S., et
535 al. (2019) SignalP 5.0 improves signal peptide predictions using deep neural networks.
536 *Nat Biotechnol* **37**: 420–423.
537 Altamia, M.A. and Distel, D.L. (2022) Transport of symbiont-encoded cellulases from the gill to
538 the gut of shipworms via the enigmatic ducts of Deshayes: a 174-year mystery solved.
539 *Proc R Soc B* **289**: 20221478.
540 Altamia, M.A., Shipway, J.R., Stein, D., Betcher, M.A., Fung, J.M., Jospin, G., et al. (2021)
541 Teredinibacter haidensis sp. nov., Teredinibacter purpureus sp. nov. and Teredinibacter
542 franksiae sp. nov., marine, cellulolytic endosymbiotic bacteria isolated from the gills of
543 the wood-boring mollusc Bankia setacea (Bivalvia: Teredinidae) and emended

544 description of the genus Teredinibacter. *International Journal of Systematic and*
545 *Evolutionary Microbiology* **71**:.
546 Altamia, M.A., Shipway, J.R., Stein, D., Betcher, M.A., Fung, J.M., Jospin, G., et al. (2020)
547 Teredinibacter waterburyi sp. nov., a marine, cellulolytic endosymbiotic bacterium
548 isolated from the gills of the wood-boring mollusc Bankia setacea (Bivalvia: Teredinidae)
549 and emended description of the genus Teredinibacter. *International Journal of*
550 *Systematic and Evolutionary Microbiology* **70**: 2388–2394.
551 Alves, N.J., Turner, K.B., Medintz, I.L., and Walper, S.A. (2016) Protecting enzymatic function
552 through directed packaging into bacterial outer membrane vesicles. *Sci Rep* **6**: 24866.
553 Arntzen, M.Ø., Várnai, A., Mackie, R.I., Eijsink, V.G.H., and Pope, P.B. (2017) Outer membrane
554 vesicles from *Fibrobacter succinogenes* S85 contain an array of carbohydrate-active
555 enzymes with versatile polysaccharide-degrading capacity. *Environmental Microbiology*
556 **19**: 2701–2714.
557 Aschtgen, M.-S., Wetzel, K., Goldman, W., McFall-Ngai, M., and Ruby, E. (2016) *Vibrio fischeri* -
558 derived outer membrane vesicles trigger host development: OMV deliver signals in the
559 squid/vibrio symbiosis. *Cellular Microbiology* **18**: 488–499.
560 Berleman, J. and Auer, M. (2013) The role of bacterial outer membrane vesicles for intra- and
561 interspecies delivery. *Environmental Microbiology* **15**: 347–354.
562 Betcher, M.A., Fung, J.M., Han, A.W., O'Connor, R., Seronay, R., Concepcion, G.P., et al. (2012)
563 Microbial Distribution and Abundance in the Digestive System of Five Shipworm Species
564 (Bivalvia: Teredinidae). *PLoS ONE* **7**: e45309.
565 Bonnington, K.E. and Kuehn, M.J. (2014) Protein selection and export via outer membrane
566 vesicles. *Biochimica et Biophysica Acta (BBA) - Molecular Cell Research* **1843**: 1612–
567 1619.
568 Brito, T.L., Campos, A.B., Bastiaan Von Meijenfeldt, F.A., Daniel, J.P., Ribeiro, G.B., Silva, G.G.Z., et
569 al. (2018) The gill-associated microbiome is the main source of wood plant
570 polysaccharide hydrolases and secondary metabolite gene clusters in the mangrove
571 shipworm Neoteredo reynei. *PLoS ONE* **13**: e0200437.
572 Burnet, M.C., Dohnalkova, A.C., Neumann, A.P., Lipton, M.S., Smith, R.D., Suen, G., and Callister,
573 S.J. (2015) Evaluating Models of Cellulose Degradation by Fibrobacter succinogenes S85.
574 *PLoS ONE* **10**: e0143809.
575 Cai, Y.J., Chapman, S.J., Buswell, J.A., and Chang, S. (1999) Production and Distribution of
576 Endoglucanase, Cellobiohydrolase, and β-Glucosidase Components of the Cellulolytic
577 System of *Volvariella volvacea* , the Edible Straw Mushroom. *Appl Environ Microbiol* **65**:
578 553–559.
579 Choi, C.-W., Park, E.C., Yun, S.H., Lee, S.-Y., Lee, Y.G., Hong, Y., et al. (2014) Proteomic
580 Characterization of the Outer Membrane Vesicle of *Pseudomonas putida* KT2440. *J*
581 *Proteome Res* **13**: 4298–4309.
582 Cragg, S.M., Beckham, G.T., Bruce, N.C., Bugg, T.D., Distel, D.L., Dupree, P., et al. (2015)
583 Lignocellulose degradation mechanisms across the Tree of Life. *Current Opinion in*
584 *Chemical Biology* **29**: 108–119.
585 Cragg, S.M., Friess, D.A., Gillis, L.G., Trevathan-Tackett, S.M., Terrett, O.M., Watts, J.E.M., et al.
586 (2020) Vascular Plants Are Globally Significant Contributors to Marine Carbon Fluxes and
587 Sinks. *Annu Rev Mar Sci* **12**: 469–497.

588 Dahmen, N., Lewandowski, I., Zibek, S., and Weidtmann, A. (2019) Integrated lignocellulosic
589 value chains in a growing bioeconomy: Status quo and perspectives. *GCB Bioenergy* **11**:
590 107–117.
591 Dhurve, G., Madikonda, A.K., Jagannadham, M.V., and Siddavattam, D. (2022) Outer Membrane
592 Vesicles of *Acinetobacter baumannii* DS002 Are Selectively Enriched with TonB-
593 Dependent Transporters and Play a Key Role in Iron Acquisition. *Microbiol Spectr* **10**:
594 e00293-22.
595 Distel, D.L., DeLong, E.F., and Waterbury, J.B. (1991) Phylogenetic characterization and in situ
596 localization of the bacterial symbiont of shipworms (Teredinidae: Bivalvia) by using 16S
597 rRNA sequence analysis and oligodeoxynucleotide probe hybridization. *Appl Environ*
598 *Microbiol* **57**: 2376–2382.
599 Distel, D.L., Morrill, W., MacLaren-Toussaint, N., Franks, D., and Waterbury, J. (2002)
600 Teredinibacter turnerae gen. nov., sp. nov., a dinitrogen-fixing, cellulolytic,
601 endosymbiotic gamma-proteobacterium isolated from the gills of wood-boring molluscs
602 (Bivalvia: Teredinidae). *International Journal of Systematic and Evolutionary*
603 *Microbiology* **52**: 2261–2269.
604 Dürwald, A., Zühlke, M., Schlüter, R., Gebbe, R., Bartosik, D., Unfried, F., et al. (2021) Reaching
605 out in anticipation: bacterial membrane extensions represent a permanent investment
606 in polysaccharide sensing and utilization. *Environmental Microbiology* **23**: 3149–3163.
607 Elhenawy, W., Debelyy, M.O., and Feldman, M.F. (2014) Preferential Packing of Acidic
608 Glycosidases and Proteases into *Bacteroides* Outer Membrane Vesicles. *mBio* **5**: e00909-
609 14.
610 Fadeev, E., Carpaneto Bastos, C., Hennenfeind, J.H., Biller, S.J., Sher, D., Wietz, M., and Herndl,
611 G.J. (2023) Characterization of membrane vesicles in *Alteromonas macleodii* indicates
612 potential roles in their copiotrophic lifestyle. *microLife* **4**: uqac025.
613 Forsberg, C.W., Beveridge, T.J., and Hellstrom, A. (1981) Cellulase and Xylanase Release from
614 *Bacteroides succinogenes* and Its Importance in the Rumen Environment. *Appl Environ*
615 *Microbiol* **42**: 886–896.
616 Galperin, M.Y., Wolf, Y.I., Makarova, K.S., Vera Alvarez, R., Landsman, D., and Koonin, E.V. (2021)
617 COG database update: focus on microbial diversity, model organisms, and widespread
618 pathogens. *Nucleic Acids Research* **49**: D274–D281.
619 Gan, Y., Zhao, G., Wang, Z., Zhang, X., Wu, M.X., and Lu, M. (2023) Bacterial Membrane Vesicles:
620 Physiological Roles, Infection Immunology, and Applications. *Advanced Science* **10**:
621 2301357.
622 Ge, S.X., Son, E.W., and Yao, R. (2018) iDEP: an integrated web application for differential
623 expression and pathway analysis of RNA-Seq data. *BMC Bioinformatics* **19**: 534.
624 Gharechahi, J., Vahidi, M.F., Sharifi, G., Ariaeenejad, S., Ding, X.-Z., Han, J.-L., and Salekdeh, G.H.
625 (2023) Lignocellulose degradation by rumen bacterial communities: New insights from
626 metagenome analyses. *Environmental Research* **229**: 115925.
627 Ghose, T.K. (1987) Measurement of cellulase activities. *Pure and Applied Chemistry* **59**: 257–
628 268.
629 Guerrero-Mandujano, A., Hernández-Cortez, C., Ibarra, J.A., and Castro-Escarpulli, G. (2017) The
630 outer membrane vesicles: Secretion system type zero. *Traffic* **18**: 425–432.

631 Hervé, C., Rogowski, A., Blake, A.W., Marcus, S.E., Gilbert, H.J., and Knox, J.P. (2010)
632 Carbohydrate-binding modules promote the enzymatic deconstruction of intact plant
633 cell walls by targeting and proximity effects. *Proc Natl Acad Sci USA* **107**: 15293–15298.
634 Huang, Y., Nieh, M., Chen, W., and Lei, Y. (2022) Outer membrane vesicles (OMVs) enabled bio-
635 applications: A critical review. *Biotechnol Bioeng* **119**: 34–47.
636 Ichikawa, S., Ogawa, S., Nishida, A., Kobayashi, Y., Kurosawa, T., and Karita, S. (2019)
637 Cellulosomes localise on the surface of membrane vesicles from the cellulolytic
638 bacterium *Clostridium thermocellum*. *FEMS Microbiology Letters* **366**: fnz145.
639 Jäckle, O., Seah, B.K.B., Tietjen, M., Leisch, N., Liebeke, M., Kleiner, M., et al. (2019)
640 Chemosynthetic symbiont with a drastically reduced genome serves as primary energy
641 storage in the marine flatworm *Paracatenula*. *Proc Natl Acad Sci USA* **116**: 8505–8514.
642 La Rosa, S.L., Ostrowski, M.P., Vera-Ponce De León, A., McKee, L.S., Larsbrink, J., Eijsink, V.G., et
643 al. (2022) Glycan processing in gut microbiomes. *Current Opinion in Microbiology* **67**:
644 102143.
645 Lombard, V., Golaconda Ramulu, H., Drula, E., Coutinho, P.M., and Henrissat, B. (2014) The
646 carbohydrate-active enzymes database (CAZy) in 2013. *Nucl Acids Res* **42**: D490–D495.
647 Lynch, J.B. and Alegado, R.A. (2017) Spheres of Hope, Packets of Doom: the Good and Bad of
648 Outer Membrane Vesicles in Interspecies and Ecological Dynamics. *J Bacteriol* **199**:.
649 McGavin, M., Lam, J., and Forsberg, C.W. (1990) Regulation and distribution of Fibrobacter
650 succinogenes subsp. succinogenes S85 endoglucanases. *Appl Environ Microbiol* **56**:
651 1235–1244.
652 Moreno, J., Nielsen, H., Winther, O., and Teufel, F. (2024) Predicting the subcellular location of
653 prokaryotic proteins with DeepLocPro.
654 Nagakubo, T., Nomura, N., and Toyofuku, M. (2020) Cracking Open Bacterial Membrane Vesicles.
655 *Front Microbiol* **10**: 3026.
656 Naka, H. and Haygood, M.G. (2023) The dual role of TonB genes in turnerbactin uptake and
657 carbohydrate utilization in the shipworm symbiont *Teredinibacter turnerae*. *Appl Environ*
658 *Microbiol* **89**: e00744-23.
659 Naval, P. and Chandra, T.S. (2019) Characterization of membrane vesicles secreted by seaweed
660 associated bacterium Alteromonas macleodii KS62. *Biochemical and Biophysical*
661 *Research Communications* **514**: 422–427.
662 O'Connor, R.M., Fung, J.M., Sharp, K.H., Benner, J.S., McClung, C., Cushing, S., et al. (2014) Gill
663 bacteria enable a novel digestive strategy in a wood-feeding mollusk. *Proc Natl Acad Sci*
664 *USA* **111**: E5096–E5104.
665 Orench-Rivera, N. and Kuehn, M.J. (2016) Environmentally controlled bacterial vesicle-mediated
666 export: Environmentally controlled bacterial vesicle-mediated export. *Cellular*
667 *Microbiology* **18**: 1525–1536.
668 Østby, H., Hansen, L.D., Horn, S.J., Eijsink, V.G.H., and Várnai, A. (2020) Enzymatic processing of
669 lignocellulosic biomass: principles, recent advances and perspectives. *Journal of*
670 *Industrial Microbiology and Biotechnology* **47**: 623–657.
671 Park, M., Sun, Q., Liu, F., DeLisa, M.P., and Chen, W. (2014) Positional Assembly of Enzymes on
672 Bacterial Outer Membrane Vesicles for Cascade Reactions. *PLoS ONE* **9**: e97103.

673 Pesante, G., Sabbadin, F., Elias, L., Steele-King, C., Shipway, J.R., Dowle, A.A., et al. (2021)
674 Characterisation of the enzyme transport path between shipworms and their bacterial
675 symbionts. *BMC Biol* **19**: 233.
676 Popham, J.D. (1974) Further observations of the gland of Deshayes in the teredo Bankia
677 australis. *Veliger* **18**: 55–59.
678 Popham, J.D. and Dickson, M.R. (1973) Bacterial associations in the teredo Bankia australis
679 (Lamellibranchia: Mollusca). *Marine Biology* **19**: 338–340.
680 Ragauskas, A.J., Beckham, G.T., Biddy, M.J., Chandra, R., Chen, F., Davis, M.F., et al. (2014) Lignin
681 Valorization: Improving Lignin Processing in the Biorefinery. *Science* **344**: 1246843.
682 Rosenberg, E., DeLong, E.F., Lory, S., Stackebrandt, E., and Thompson, F. eds. (2014) The
683 Prokaryotes: Gammaproteobacteria, Berlin, Heidelberg: Springer Berlin Heidelberg.
684 Sabbadin, F., Pesante, G., Elias, L., Besser, K., Li, Y., Steele-King, C., et al. (2018) Uncovering the
685 molecular mechanisms of lignocellulose digestion in shipworms. *Biotechnol Biofuels* **11**:
686 59.
687 Salvachúa, D., Werner, A.Z., Pardo, I., Michalska, M., Black, B.A., Donohoe, B.S., et al. (2020)
688 Outer membrane vesicles catabolize lignin-derived aromatic compounds in
689 *Pseudomonas putida* KT2440. *Proc Natl Acad Sci USA* **117**: 9302–9310.
690 Sartorio, M.G., Pardue, E.J., Scott, N.E., and Feldman, M.F. (2023) Human gut bacteria tailor
691 extracellular vesicle cargo for the breakdown of diet- and host-derived glycans. *Proc Natl*
692 *Acad Sci USA* **120**: e2306314120.
693 Schwechheimer, C. and Kuehn, M.J. (2015) Outer-membrane vesicles from Gram-negative
694 bacteria: biogenesis and functions. *Nat Rev Microbiol* **13**: 605–619.
695 Solé, M., Scheibner, F., Hoffmeister, A.-K., Hartmann, N., Hause, G., Rother, A., et al. (2015)
696 Xanthomonas campestris pv. vesicatoria Secretes Proteases and Xylanases via the Xps
697 Type II Secretion System and Outer Membrane Vesicles. *J Bacteriol* **197**: 2879–2893.
698 Spring, S., Scheuner, C., Göker, M., and Klenk, H.-P. (2015) A taxonomic framework for emerging
699 groups of ecologically important marine gammaproteobacteria based on the
700 reconstruction of evolutionary relationships using genome-scale data. *Front Microbiol* **6**:.
701 Szklarczyk, D., Gable, A.L., Lyon, D., Junge, A., Wyder, S., Huerta-Cepas, J., et al. (2019) STRING
702 v11: protein–protein association networks with increased coverage, supporting
703 functional discovery in genome-wide experimental datasets. *Nucleic Acids Research* **47**:
704 D607–D613.
705 Teather, R.M. and Wood, P.J. (1982) Use of Congo red-polysaccharide interactions in
706 enumeration and characterization of cellulolytic bacteria from the bovine rumen. *Appl*
707 *Environ Microbiol* **43**: 777–780.
708 Thakur, M., Dean, S.N., Caruana, J.C., Walper, S.A., and Ellis, G.A. (2023) Bacterial Membrane
709 Vesicles for In Vitro Catalysis. *Bioengineering* **10**: 1099.
710 Toyofuku, M., Schild, S., Kaparakis-Liaskos, M., and Eberl, L. (2023) Composition and functions of
711 bacterial membrane vesicles. *Nat Rev Microbiol* **21**: 415–430.
712 Veith, P.D., Chen, Y.-Y., Chen, D., O'Brien-Simpson, N.M., Cecil, J.D., Holden, J.A., et al. (2015)
713 Tannerella forsythia Outer Membrane Vesicles Are Enriched with Substrates of the Type
714 IX Secretion System and TonB-Dependent Receptors. *J Proteome Res* **14**: 5355–5366.
715 Voight, J.R. (2015) Xylotrophic bivalves: aspects of their biology and the impacts of humans.
716 *Journal of Molluscan Studies* **81**: 175–186.

717 Waterbury, J.B., Calloway, C.B., and Turner, R.D. (1983) A Cellulolytic Nitrogen-Fixing Bacterium
718 Cultured from the Gland of Deshayes in Shipworms (Bivalvia: Teredinidae). *Science* **221**:
719 1401–1403.
720 Yan, S. and Wu, G. (2013) Secretory pathway of cellulase: a mini-review. *Biotechnol Biofuels* **6**:
721 177.
722 Yang, J.C., Madupu, R., Durkin, A.S., Ekborg, N.A., Pedamallu, C.S., Hostetler, J.B., et al. (2009)
723 The Complete Genome of Teredinibacter turnerae T7901: An Intracellular Endosymbiont
724 of Marine Wood-Boring Bivalves (Shipworms). *PLoS ONE* **4**: e6085.
725 Zakharzhevskaya, N.B., Vanyushkina, A.A., Altukhov, I.A., Shavarda, A.L., Butenko, I.O., Rakitina,
726 D.V., et al. (2017) Outer membrane vesicles secreted by pathogenic and nonpathogenic
727 Bacteroides fragilis represent different metabolic activities. *Sci Rep* **7**: 5008.
728 Zhang, B., Jia, C., Li, M., Wang, K., Chen, J., and Zhao, J. (2024) Multiomics integration for the
729 function of bacterial outer membrane vesicles in the larval settlement of marine
730 sponges. *Front Microbiol* **15**: 1268813.
731 Zingl, F.G., Thapa, H.B., Scharf, M., Kohl, P., Müller, A.M., and Schild, S. (2021) Outer Membrane
732 Vesicles of Vibrio cholerae Protect and Deliver Active Cholera Toxin to Host Cells via
733 Porin-Dependent Uptake. *mBio* **12**: e00534-21.
734